NISS

A Comparison of Regional Oxidant Model (ROM) Output with Observed Ozone Data

J. M. Davis, D. Nychka, and B. Bailey

Technical Report Number 85
May, 1998

National Institute of Statistical Sciences
19 T. W. Alexander Drive
PO Box 14006
Research Triangle Park, NC 27709-4006
www.niss.org

A Comparison of Regional Oxidant Model (ROM) Output with Observed Ozone Data

J. M. Davis
Departments of Marine, Earth & Atmospheric Sciences
North Carolina State University, Raleigh, NC and
National Institute of Statistical Sciences, Research Triangle Park, NC

D. Nychka
Department of Statistics
North Carolina State University, Raleigh, NC and
National Institute of Statistical Sciences, Research Triangle Park, NC

B. Bailey
National Center for Atmospheric Research, Boulder, CO

21 May 1998

Abstract

The output from the Regional Oxidant Model (ROM) is compared to observed ozone over Northern Illinois for June, July and August 1987. The 8-hour daily average at the ozone monitoring stations is interpolated to the ROM grid cells using a spatial statistical method. Differences between the model output and spatial predictions are compared at three levels of spatial averaging (grid cell, 6×6 block , 4 blocks) and three levels of temporal averaging (daily, weekly, 3 months). In addition two monitoring stations are paired with weather stations and ROM cells in order to investigate the performance of ROM as a function of meteorological conditions. For daily values the root mean squared

error (RMSE) between the ROM values and those predicted from the monitoring network varies between 14 and 25 PPB with the largest discrepancies occurring near Lake Michigan. Weekly averages reduce the RMSE by approximately 30% but spatial aggregation is not helpful in improving the agreement. The difference between ROM and the two paired sites depends most strongly on temperature and to a lesser extent on dew point temperature. The R^2 from linear regressions is approximately 35% . Typically ROM is found to over predict ozone under cool, cloudy conditions. An examination of the synoptic-scale and meso-scale weather patterns during this period indicates that ROM is sensitive to dynamic situations such as a frontal passage.
KEY WORDS: Ozone, Model Validation

1 Introduction

The Regional Oxidant Model (ROM) has been developed as a tool for predicting the effect of different emission patterns on the production of ambient ozone (U.S. EPA, 1991). Because policy decisions may be partly based on the results of this model, it is important to confirm its accuracy in modeling actual pollutant concentrations. Also it is important to identify meteorological conditions and spatial regions where the model is not reliable.

In this work the model output for the months June, July and August of 1987 is compared to ozone measured by the NAMS/SLAMS monitoring network for the Northern half of Illinois. Although this analysis is limited in its regional scope, we investigate the effect of different levels of spatial and temporal aggregation on the ROM results. This strategy could serve as a blueprint for a more comprehensive study of ROM for the Eastern United States.

The next section describes ROM and the previous work on its validation. Section 3 discusses the observational ozone measurements and the method used to interpolate the sparse irregular observational network to the regular ROM grid. This procedure is commonly used in geostatistics and includes an estimate of the error

in interpolation. Section 4 presents the comparison of the ROM and observational data at different space and time scales and Section 5 reports the dependence on meteorology. The last section is a discussion of these results.

2 The Regional Oxidant Model

Using meteorology and precursor emissions as the driving elements, the EPA regional oxidant model (ROM) can be used to infer ozone concentrations for the Eastern United States. This is a boundary layer photochemical grid model with a resolution that is useful for modeling large (1000 km) domains. The model attempts to simulate ozone under different emission inputs and different meteorology. ROM will be most useful for studying the effect of hypothetical emission patterns on the production of ozone. However, for validation it is necessary to set the inputs to match specific time periods where observational data is available. The simulation run studied here is based on results from ROM (version 2.2), where emissions and weather inputs have been set to follow the "ozone season" for 1987, 6/3/1987- 8/30/1987. The model output is on a grid with a spacing of 1/4° latitude by 1/6° longitude (18.5 km $\times$ 18.5 km) and hourly values for ozone are available for each grid cell. Throughout this work the ROM output variable for ozone will be interpreted as the integrated value in the grid cell.

2.1 Previous work on model validation

The work of Chu (1995a, 1995b, and 1996) has made an extensive comparison of ROM output to monitoring station data over the simulation period July 3 - 10 1988. Specifically he used the four closest ROM grid cells to predict ozone for each monitoring station operating in this period. These paired differences were then summarized over three levels of spatial aggregation and three levels of time aggregation to investigate the average performance of the model. Typically he finds that the root mean squared error of the *maximum* value of ozone ranges from 11 to 40 PPB

for the midwest region of his study over the eight days of the model run. His general conclusion is that ROM performs reasonable well during this period. Although the accuracy is not high for fine spatial and temporal scales, the agreement is acceptable if the temporal aggregation is at least 9 hours and the spatial aggregation is over a 10×10 (185 km $\times$ 185 km) box.

Due to the way the observational data is matched to ROM output, this study is limited to the scattered ROM cells that are close to monitoring stations. Also, the comparison focuses on the maximum value of ozone in a time window, and does not address other daily summaries.

2.2 ROM output

As a complement to Chu's work we have considered the detailed resolution of ROM performance for a region that includes the Chicago metropolitan area and extends to most of northern and central Illinois. Our interest is to determine the higher limits of ROM resolution, and so to make the comparison manageable, we have restricted attention to a small part of the model domain. The study region comprises 144 ROM grid cells arranged in 4 blocks of $36 = 6 \times 6$ cells (see Figure 1). The first block (Block 1) contains the Chicago urban area and part of Lake Michigan. The remaining three blocks (Blocks 2-4) are arranged in a North to South line and extend into the middle and more rural part of Illinois. To avoid the problems of shifts in the diurnal cycle the comparison has been restricted to a daily summary of ozone: the 8-hour average from 9AM-5PM. Because ozone typically peaks in the early afternoon, this fixed 8-hour average will be close to the maximum 8-hour average. In 1997 the 1-hour primary standard was replaced by an 8-hour standard at the level of 80 ppb based on the 3-year average of the annual fourth-highest 8-hour average concentration measured at each monitor within an area.

3 Observational Data

Average ozone values for the ROM grid cells were predicted from approximately 150 ozone monitoring stations from a larger region that contains the ROM study cells. The station data are available from AIRS, the EPA air quality data base. Locations of the stations are indicated in Figure 1. Not all of the stations have full data records, and missing hourly values were imputed using a median polish technique (Bloomfield et al., 1996).

It is important to model the observed ozone field carefully in order to obtain accurate spatial prediction *and* valid standard errors for these predictions. Usual spatial models that assume a stationary covariance are not appropriate for ozone and so we were lead to nonstationary models. The software (FUNFITS) used for the calculations outlined below is described in Nychka et al. (1998).[1]

One simple departure from nonstationarity is to consider a spatial process that has different marginal variances but isotropic correlations. Specifically, let $Y(\boldsymbol{x})$ denote the value of ozone at location $\boldsymbol{x}$ and assume that $EY(\boldsymbol{x}) = \mu(\boldsymbol{x})$ and $VAR(Y(\boldsymbol{x})) = \sigma(\boldsymbol{x})^2$. Thus, μ and σ are the marginal mean and standard deviation for the spatial process. Now consider the standardized process

$$Z(\boldsymbol{x}) = \frac{Y(\boldsymbol{x}) - \mu(\boldsymbol{x})}{\sigma(\boldsymbol{x})}$$

The key assumption is that this new process is isotropic. In particular assume that $Z(\boldsymbol{x}_k) = f(\boldsymbol{x}_k) + e_k$ where f has an exponential covariance kernel,

$$COV(f(\boldsymbol{x}), f(\boldsymbol{x}')) = \rho_f e^{-d/\theta}$$

Here d is the great circle distance between $\boldsymbol{x}$ and $\boldsymbol{x}'$ and $\{e_k\}$ are assumed to have mean zero, and to be uncorrelated with variances ρ_e.

The estimates for the ozone field under this setup are easy. If μ and σ are known one standardizes the observed data, computes the spatial process estimate

[1] Also see the Funfits web page: http://www.stat.ncsu.edu/ nychka/funfits/

for the standardized, isotropic process and applies the inverse transform to obtain predictions for the original process. That is, $\hat{Y}(\boldsymbol{x}) = \hat{Z}(\boldsymbol{x})\sigma(\boldsymbol{x})+\mu(\boldsymbol{x})$. The standard errors for $\hat{Y}(\boldsymbol{x})$ are those derived for Z multiplied by $\sigma(x)$. [2]

Although this model is only an approximate fit to the variogram of the observed covariance function, it is adequate for the moderate and short distances needed for the spatial interpolation. For all the days in the model period, the range parameter, θ, of the covariance function was fixed at $\theta = 343$ miles. The mean and standard deviation surfaces were estimated using a thin plate spline fit to the sample means and standard deviations observed over the study period (89 days) at the ozone monitoring sites. However, the values for ρ_f and ρ_e were estimated for each day individually using cross-validation. This flexibility allows for a modest degree of adaptation of the covariance model to the ozone field on each different day. For conciseness the functional estimate from this procedure will be referred to as the *interpolated* surface. However, if $\rho_e > 0$ some smoothing will be applied to the observed data resulting in a surface that does not pass through the observed points exactly. For the 89 days of the model run the estimated values of ρ_e for the ozone field had a mean of 2.33 and ranged from .037 to 8.83. This indicates substantial variability from day to day in the roughness of the ozone field and is illustrated by the three days in Figure 5.

Using the estimated surface, the integration over the ROM cells is approximated by taking the mean over a 10×10 mesh of points. This approximation simplifies the computations and seems reasonable since this grid spacing will be less than 2 km. The standard error of this estimate is found by first computing the covariance matrix for the 100 point mesh and using the standard formula for the variance of a linear combination of dependent random variables (see Figure 2).

[2] In this work we are avoiding the more difficult problem of adjusting the prediction standard errors for the fact that μ and σ are estimated and not known precisely. This is justified because they are averages over the whole study period and so we expect them to have significantly less variability than the daily surface predictions.

4 Comparison of Model Output to Observational Data

In this section the *predicted* values will refer to those derived from observational data. Specifically the predictions are the average ozone summary for a ROM grid cell obtained as a result of spatial interpolation of the monitoring network. Following the work of Chu cited above, the difference between the predicted summaries and those generated from the ROM output will be analyzed at several scales. For spatial aggregation we consider averages over:

1. ROM grid cells (144)
2. 6×6 blocks of grid cells (4)
3. Entire study region. (1)

With respect to time, averages are calculated for

1. Daily values (89)
2. Weekly values (12)
3. Entire ozone season (1)

The number of averages at each of these levels is indicated in parentheses and so the total number of differences for any combination of space and time levels is the product of the two numbers. The results for these different combinations are organized by the level of spatial aggregation.

4.1 First level: ROM grid cells

Let O_{tj} denote the ROM daily ozone summary for day t and ROM cell j and $\hat{O}_{tj}$ the corresponding prediction. Differences will be calculated as

$$O_{tj} - \hat{O}_{tj}$$

while relative differences are

$$(O_{tj} - \hat{O}_{tj})/O_{tj}$$

Another weighted difference is to adjust $O_{tj} - \hat{O}_{tj}$ by the accuracy of the spatial prediction. Letting σ_{tj}^2 denote the (estimated) prediction variance of $\hat{O}_{tj}$ this leads to a standardized difference

$$(O_{tj} - \hat{O}_{tj})/\sigma_{tj}$$

Because the covariance function is estimated separately for each day, the prediction standard errors will vary over both time and space. Under this normalization, if the ROM values were derived from the same ozone field sampled by the network, then the standardized differences should have a mean of 0 and variance of 1.

4.2 Comparison of the daily performance of ROM

Figure 3 illustrates the distribution of the ordinary and relative differences between ROM and predicted values over time for each ROM cell. There is some variability in the distribution of the difference between summaries and predicted values for different days. Note for example the wide range of values on days 16 (18 June) and 17 (19 June) compared with a significantly lower variability in the period of days 23-26 (25-28 June). These are also apparent with respect to relative differences. Standardized differences are plotted in Figure 4. Based on the reference lines at ± 2 there is evidence that much of the variability for the differences on days 16 and 17 can not be attributed to the statistical method used to derive predicted values.

Figure 5 gives the paired ROM output and interpolated ozone surfaces for three different days (16, 17 and 41 (13 July)). Based on the observational data, day 16 has high ozone over the Chicago area and lower part of Lake Michigan. There are no data over the lake. Although the ROM output for this day also indicates elevated ozone values in the range of 70-80 PPB in this region, they are large underestimates of the predicted values. On day 17 there is an overestimate by ROM in the Chicago area (Block 1). The ROM output creates a peak in ozone of 120 PPB over Chicago and

a sharp decrease over Lake Michigan. This is in contrast to the smooth and much lower (80-90 PPB) predicted surface. The last day in this panel gives an example of very a low (< 30 PPB) ozone field. This is matched by a ROM field that also exhibits low concentrations of ozone but not as low as the observational values. Because the formation of ozone is highly dependent on meteorological conditions, an examination of how conditions varied spatially and temporally over these time periods should help to shed some light on the results obtained. Large-scale meteorological conditions are outlined in the following paragraphs.

To the north of Illinois a cold front stretched from Lake Superior through southern Minnesota into Kansas and Nebraska on day 16. By the day 17 this front had become stationary and stretched from central Michigan through Wisconsin and Iowa into Nebraska and Kansas. On day 16 the tail end of another front (stationary in this case) was located in southern Illinois; by day 17 this stationary front had weaken somewhat. The meteorological conditions across Illinois were uniform, but different, on both days. On day 16, the skies across Illinois were partly cloudy. There was an increase of cloud cover across the state on day 17. Afternoon temperatures on day 16 ranged from the mid 80s to the low 90s while on day 17 they ranged from the low to high 80s. Dew points on both days ranged from the low 60s to the low 70s. Winds across the state were mostly from the south through southeast on both days. No large-scale precipitation events were reported on either day.

Based on the these synoptic-scale events, and how the model developers have described the performance of ROM under such conditions, one would expect ROM and the observed ozone values to be comparable on day 16. Figure 5 indicates that ROM values were generally less than the observed ozone values in most areas of the state. This relationship is also indicated in Figure 14 which shows the hourly ROM and observed ozone data for Peoria. Figure 15 shows the hourly Peoria meteorological data.

Given the change in the cloud conditions on day 17, one would expect to see

observed ozone values and ROM values comparable to each other in the northern part of the state, while in the southern part of the state, ROM would be expected to over predict. To some extend this is what occurred (see Figure 5). The Peoria data in Figure 14 appears to confirm the over prediction. See Figure 15 for the meteorological data.

On day 41 a cold front stretched across Illinois from the tip of Lake Michigan through the St. Louis area into southeastern Missouri. It was mostly cloudy across the state with rain showers being reported at several locations. Afternoon temperatures were cooler in the northern part of the state (upper 60s) behind the front and somewhat warmer (lower 70s) in the southern part of the state in advance of the front. Winds across the state were mainly from the northwest, even in advance of the front because of the prior passage of a trough line.

These synoptic conditions are in general not favorable for ozone formation. In addition, under these conditions, ROM tends to over predict. The spatial plot in Figure 5 indicates this over prediction, and it is confirmed by the Peoria hourly ozone data for this day (see Figure 14). Figure 16 indicates the cool, cloudly conditions at Peoria on this day.

4.3 Spatial comparisons

Next we consider the distribution of errors by collapsing over time. The root mean squared error for each ROM cell can be estimated by

$$RMSE_j = \sqrt{\frac{1}{89} \sum_{t=1,89} (O_{tj} - \hat{O}_{tj})^2}$$

and root mean squared *relative* error is

$$RMRSE_j = \sqrt{\frac{1}{89} \sum_{t=1,89} \left(\frac{(O_{tj} - \hat{O}_{tj})}{O_{tj}} \right)^2}$$

The estimated bias is given by

$$BIAS_j = 1/89 \sum_{t=1,89} (O_{tj} - \hat{O}_{tj})$$

Figure 6 plots these measures of agreement as a function of spatial location. Clearly there are consistently large differences in the grid cells over Lake Michigan. The last contour plot is the root mean squared error adjusted by the average prediction variance. Let

$$adjRMSE_j^2 = RMSE_j^2 - 1/89 \sum_{t=1,89} \sigma_{tj}^2$$

Under the assumption that O_{tj} are uncorrelated over time, the adjusted RMSE can be interpreted as the variability above that expected from just the interpolation method.

The effect of temporal averaging is indicated by the set of boxplots in Figure 7. The first boxplot gives the distribution of $RMSE_j$. The root mean squared errors for the weekly averages are calculated in a similar way to that done before, except that weekly average summaries are substituted for the daily summaries, and so instead of 89 values there are only 12. The RMSE for the seasonal averages are the same as $|BIAS_j|$. Here we see that weekly averages give some reduction in the variability of the differences.

4.4 Block averages

A qualitative summary of the block averages is given by the panel of time plots in Figure 8. Table 1 reports the RMSE errors for each block. For the block averages there is at least a 50% decrease in RMSE going from daily to weekly averages. Except for Block 1 the bias constitutes a smaller fraction of the MSE than the variance. The reduction in RMSE going from block averages to the entire study region is small.

	Daily RMSE	Bias	Weekly RMSE
Block 1	17.89	11.04	12.01
Block 2	12.99	2.21	7.25
Block 3	13.39	4.39	8.16
Block 4	13.07	5.76	8.75
Study region	12.73	5.85	8.30

Table 1: Root mean squared errors associated with the four 6×6 blocks of ROM cells from Figure 1.

4.5 Study region

The final level of spatial averaging is over all 144 ROM cells that comprise the study region. The last time plot in Figure 8 summarizes the agreement between the predicted average and ROM output over time. The RMSE for the differences have also been reported in Table 1. Note that the absolute value of the bias term reported in this table is also equal to the absolute difference between the ROM average over the season and study region minus the same average based on predictions. Finally Figure 9 indicates the functional relationship between the ROM output and the predicted ozone for the study region. The line drawn at 45° indicates that the ROM average is consistently below the predicted value. Moreover the curve fit by a smoothing spline suggests a nonlinear relationship between these two variables. As a reference for Figure 5 note that the days 15, 16 and 41 are unusual ones and lie on the boundaries of the point cloud.

5 Quantitative Dependence on Meteorology

The effect of meteorological conditions on the accuracy of ROM output was investigated by pairing ROM cells with individual monitoring stations. The monitoring stations were selected to be close to a first order National Weather Service observing

station and the ROM grid cell was taken to be the one containing the ozone station. This was done to avoid the added error due to interpolation and took advantage of the close proximity of the ozone and weather stations. The analysis was done for two pairs. The first uses a ROM cell and ozone station in the first block and the second pairing is inland from the Lake Michigan in the third block. In addition to working with daily summaries, two time periods were selected for closer scrutiny and hourly data were examined.

5.1 Meterological data

The meteorological variables used in the regression model were:

1. Average temperature (temp), C
2. Average dew point temperature (tdew), C
3. Average wind speed (wspd), m/s
4. Average u,v component wind speed (ucom, vcom), m/s
5. Average total cloud cover (tcov), in tenths
6. Average opaque cloud cover (ocov), in tenths
7. Average global radiation (hrad), W/m^2
8. Average station pressure (pres), mb
9. One-day lagged values for selected variables.

When the meteorological data were averaged, the same 8-hour time period was used as for the ozone data.

5.2 O'Hare Airport station

The first comparison was made for a station pair near the National Weather Service station (41.983N, 87.9W) at the Chicago O'Hare Airport (see point labeled OH on Figure 1). The ROM cell (97,45) contained both the observed ozone site (41.668N, 87.990W) and O'Hare Airport. Figure 10 gives time plots of the ROM output and observed ozone for the 89-day period. For much of the period, ROM tends to be greater than the observed ozone and in particular over-estimates troughs in the observed series.

The difference (ROM - predicted) was regressed on the meteorological data from the airport. Although several different approaches were taken for model selection, the final analysis is based on a linear model where the subset of regression variables was chosen by forward stepwise selection. Of the eight variables and their lags, only temp (negative coefficient) and tdew (positive coefficient) were significant at the 5 % level (see Figure 11). The R-squared value was 0.375 with a residual standard deviation of 14.5 PPB. However, because of the high degree of correlation (temp/tdew, 0.58; tcov/hrad, -0.78; temp/hrad, 0.5) among the meteorological variables, it is difficult to identify a single best model.

The regression model indicates that at lower temperatures ROM ozone summaries are larger than those observed. These would, on average, tend to be either times with cloud cover and low radiation input or relatively clear conditions that occurred after a frontal passage. At higher temperatures, ROM appeared to be very close to the observed values. Such conditions would be associated with clear, warm summer days.

At low dew points, ROM produced good predictions. Low dew points would tend to occur either on warm clear summer days or on days just after a frontal passage. ROM gave a less accurate predictions on days with high dew points. Typically these days have high cloud cover levels.

5.3 Peoria stations

The second comparison was made in central Illinois away from both the synoptic- and meso-scale (lake breeze effect) influence of Lake Michigan. Two ozone observation locations: Peoria South (40.688N, 89.608W) and Peoria North (40.746N, 89.586W), points `PN` and `PS` on Figure 1, were paired with the Peoria National Weather Service station (40.667N, 89.683W). The weather station is located on the boundary of the ROM cell. As indicated by the latitude/longitude, the North and South stations were within several kilometers of each other. Figure 12 is a panel of time plots of these stations' data, their average and the ROM data series. The sample correlation coefficient for South and North was 0.96, and results will be presented based on the difference between the ROM ozone summary and the average of the two Peoria stations.

The meteorological variables 1-3 and 5-8 were used in the analysis and again a stepwise linear model approach was preferred. Temp (negative coefficient), tdew (positive coefficient) and wspd (positive coefficient) were significant at the 5% level. The R^2 in this case was .346 with a residual standard deviation of 12.6 PPB. Figure 13 contains plots of ROM minus the average observed value versus temperature, dewpoint and wind speed. The patterns for temperature and dewpoint are similar to the results for the O'Hare Airport pair. In addition there is a weak dependence on wind speed. At Peoria, ROM tended to over-predict as wind speed increased.

5.4 Hourly data for Peoria

Figure 12 was used to select two time periods for closer examination. The days 10-20, 12 June to 22 June, were selected as a period where the ROM output tended to be lower than the observed ozone record. In contrast the period 33-43, 5 July to 15 July, was selected because ROM tended to be higher than the observed ozone. Figure 14 shows time series plots for both the June and July periods.

Most of the June period is characterized by ROM amplitude and phase conditions

that matched the observed data. The most notable departure from this agreement is for days 13-15. Here the ROM time series does not exhibit a normal diurnal maximum in the mid afternoon but increases throughout the day.

The July period is characterized by ROM over prediction coupled with what appears to be nocturnal peaks in ozone on day 35. The most extended interval of over prediction occurs from day 40 to 43. The 8-hour averages also reflects this pattern during these ten days. A description of the meteorology for each period follows.

Figures 15 and 16 show the hourly meteorological conditions for the June and July periods, respectively. An examination of the meteorological conditions for days 13-15 indicated that leading up to day 14 (about 4 days into the period) there was a dramatic drop in the dew point (tdew), an increase in the wind speed (wspd), mostly cloudy conditions (tcov), and a wind shift (wdir) from the northwest to the northeast. Synoptic weather maps indicated that during this period a weak cold front passed through the Peoria area from the north bringing cooler, drier conditions. All the observed conditions shown in Figure 15 were consistent with this event. This front remained in the area for the next several days.

The period after day 17 (19 June) was characterized by cloudy, cool conditions. During this period there were a number of weak frontal systems and weak low pressure systems in the region.

The July period appears to be the result of general overforecasting by ROM. Problems arose early in the period (day 34, 6 July) when the observed ozone had low daytime levels followed by high night time ones. The ROM forecast for day 34 was well over the observed daytime high. ROM then under-predicted the nighttime ozone by a substantial amount. Meteorological conditions in the region were dominated by a short wave trough bringing cool, partly cloudy conditions. Winds remained from the south to southwest during this period. The reason for the high nighttime ozone level is unknown.

Days 37 and 38 (9 and 10 July) were interesting because the 8-hr averages indicated over predictions by ROM, while the hourly data seemed to match one of the observed stations rather well. During these two days the area was under the influence of high pressure. Maximum temperatures were about 32C under partly cloudy skies.

Beginning on day 40 (12 July) a period was entered where ROM over-predicted for an extended period of time, and the two observed ozone stations were in close agreement. It was also a period of changing weather conditions. The maximum temperature on day 39 (11 July) was about 34C. A cold front moved through the area on 13 July. Maximum temperatures from 12-15 July were in the mid- 20s. It was generally cloudy except for a brief period of time after the frontal passage. The area then came under the influence of a weak trough on 15 July and the cloud cover returned.

6 Discussion and Conclusions

At a temporal resolution of 24 hours and spatial scale of a single grid cell there are some large discrepancies between model output and the observational ozone. Even when prediction error is taken into account (Figure 2) there are still large biases and mean squared errors in the differences. As might be expected the largest root mean squared errors (approximately 20-25 PPB) occurred over Chicago and Lake Michigan where lake breezes and other complex influences from the Lake make modeling ozone production and transport difficult. There is much better agreement in central Illinois away from lake influences and the bias between ROM ozone and the predictions is a smaller fraction (20%) of the total mean squared error. The low mean squared errors (10 - 14 PPB) are surprising given the sparseness of the monitoring network in this area and the difficulty in predicting the ozone field. One possible explanation is that the ozone field is much smoother over these rural areas, and thus it is simpler to model and easier to predict ozone from a limited number of

observation sites. This feature may also explain lower biases. Overall the accuracy of ROM in this study is lower than Chu's results. This result is not surprising since he used the daily maximum as a summary which has more variability than an 8-hour average.

As might be expected, averaging over time decreases the root mean squared error. For example the median RMSE for the grid cells decreases by approximately 40% from 14.85 PPB for daily values to 8.60 PPB for weekly averages. If the daily values were independent, one would expect a reduction by multiplication by the factor $1/\sqrt{7}$. Even if the prediction error is accounted for this reduction is not realized and suggests some positive dependence among the daily differences. Another component could be persistent biases in the model that are not decreased by averaging over time.

For most of the study region, spatial averaging is not effective in improving the agreement between the model and observational data. The RMSE for the block averages are comparable to the individual grid cells for blocks 2- 4. However, there is some benefit for the first block where the RMSE is reduced by approximately 33% for grid cells situated over Lake Michigan.. Even in this case the actual reduction is far from the naive expectation of a factor of $1/6 = 1/\sqrt{36}$ under the assumption of independent grid cells. In fact, from other work we have found that the correlation among adjacent ROM cell is in the range (.8 - .95). Such high spatial correlations will thwart the reduction in variability due to averaging. The pair-wise analysis to find dependence on meteorological variables confirms what was already known about ROM; namely, it does not do well under cool, cloudy conditions. The linear relationships are not strong however and only explain about 35% of the variance in the differences.

Note that the regression analysis attempts to find meteorological dependence on the *difference* between the modeled and observed ozone. If ROM was making optimal use of meteorology in modeling ozone, then the differences should not exhibit any

dependence on meteorological variables. The weak dependence found in our analysis suggests that ROM is not missing some simple correction due to meteorological variables. Based on the synoptic analysis of the data at Peoria there does seem to be problems with the model adjusting to rapidly changing conditions, such as the passage of a front. This inaccuracy of the model may help to explain why improvements in the mean square error are seen for weekly averages. A 7-day average would be less sensitive to dynamic conditions.

7 References

Bloomfield, P, Royle, J.A., Steinberg, L.J. and Yang, Q. 1996. Accounting for meteorological effects in measuring urban ozone levels and trends. Atmospheric Environment 30: 3067-3077.

Chu, S-H, 1996. ROM2.2 model performance in the July 3-11, 1988 ozone episode. Proceedings of the 1996 AMS-AWMA Joint Meeting.

Chu, S-H, 1995a. Partition of phase and magnitude contributions in residual variance analysis. Journal of Geophysical Research 100:18639-18649.

Chu, S-H, and Cox, W.M. 1995b. Effects of emissions reductions on ozone predictions by the Regional Oxidant Model during the July 1988 episode. Journal of Applied Meteorology 34:679-693.

Cressie, N. 1993. Statistics for Spatial Data. New York: John Wiley and Sons. 900 pp.

Nychka, D, Piegorsch, W.W., and Cox, L.H. 1998 (forthcoming). Case Studies in Environmental Statistics. New York: Springer. 192 pp.

U.S. EPA 1991. The Regional Oxidant Model (ROM). Part I: User's Guide. U.S. EPA Report EPA-600/8-90/083a.

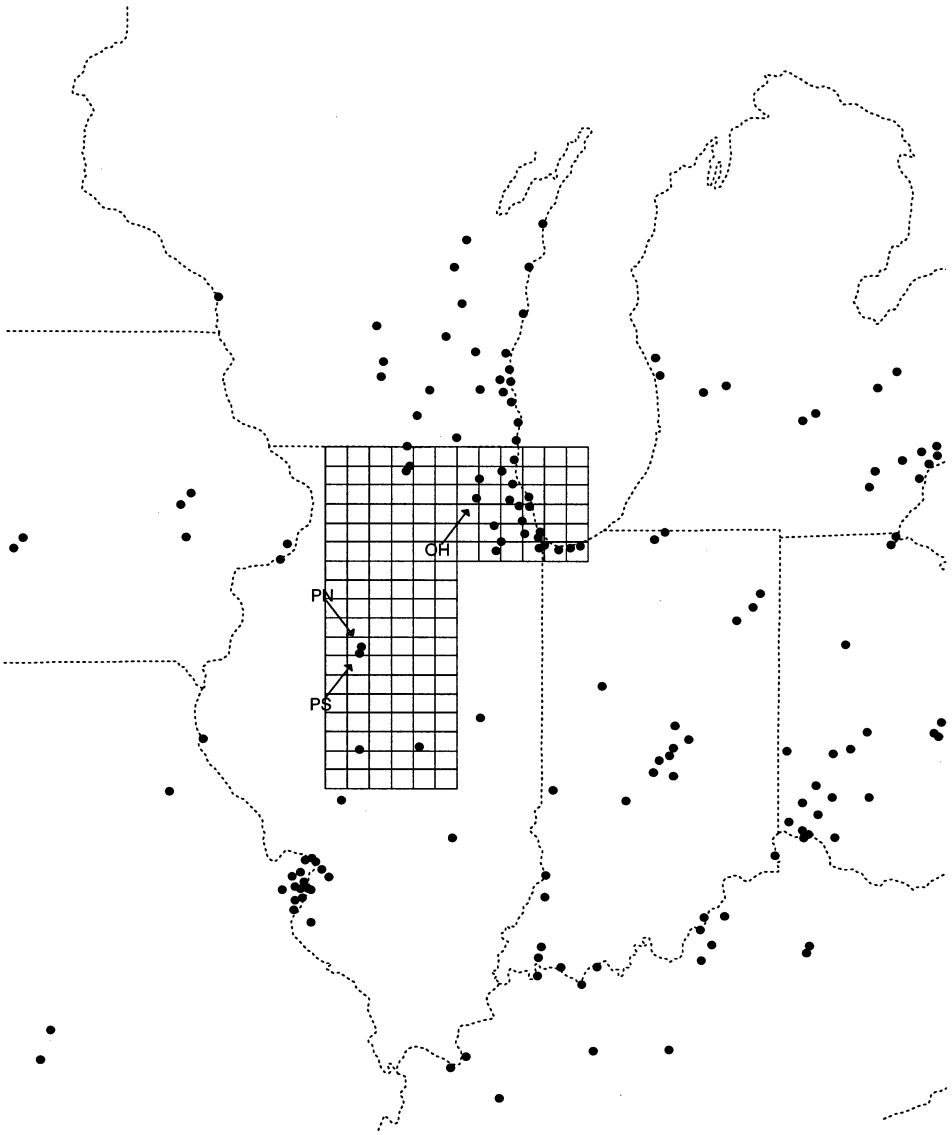

Figure 1: ROM Study Region.

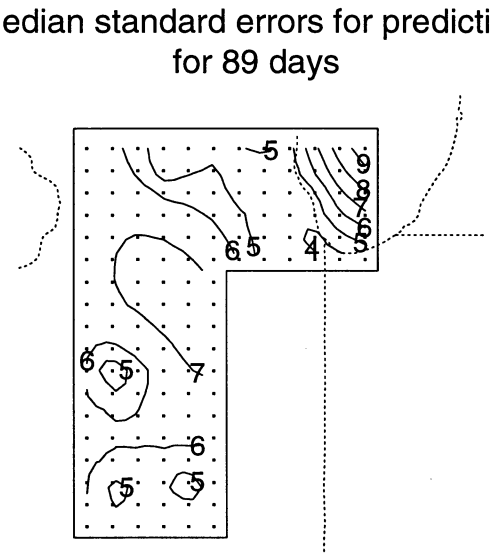

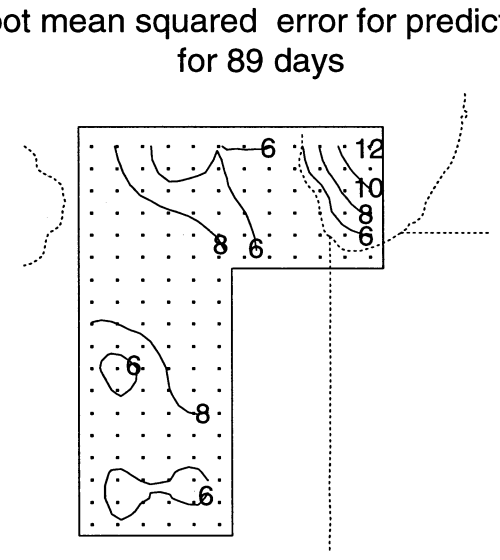

Figure 2: Standard errors for the prediction surface.

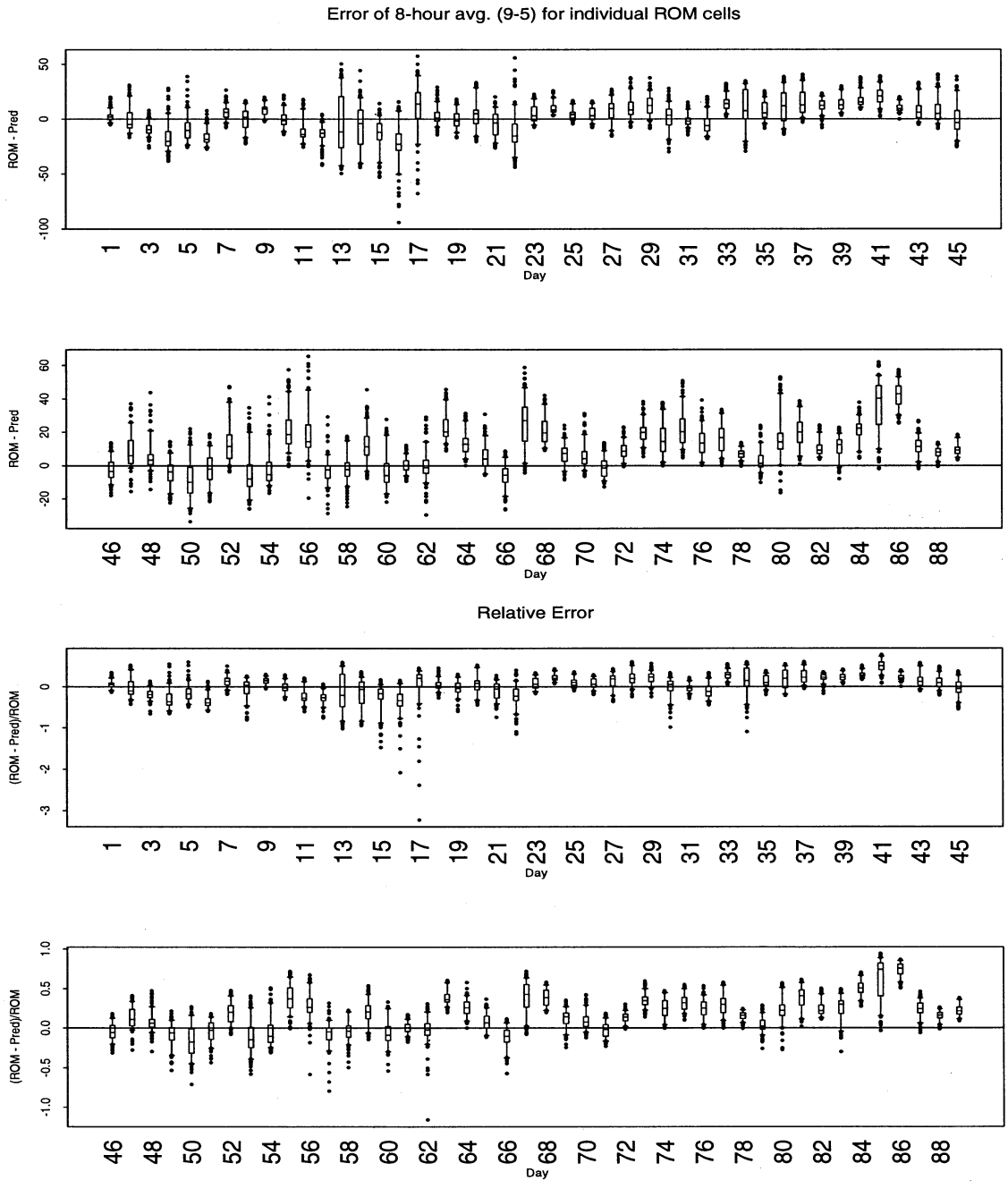

Figure 3: Boxplots of grid cell differences by day.

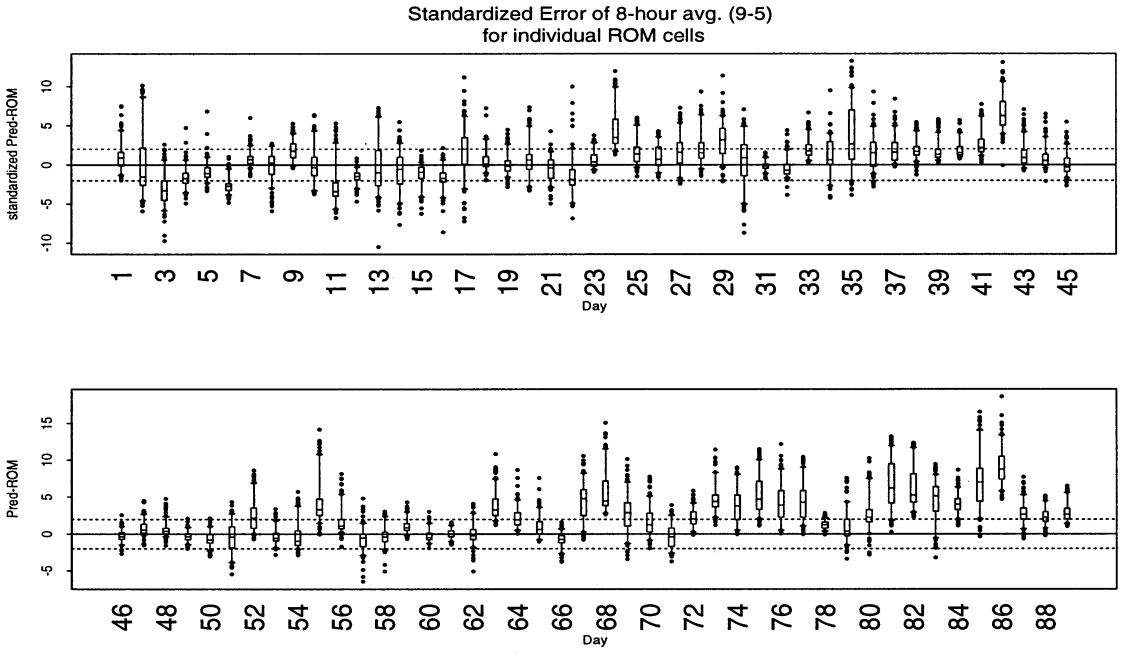

Figure 4: Boxplots of grid cell differences divided by the prediction standard errors.

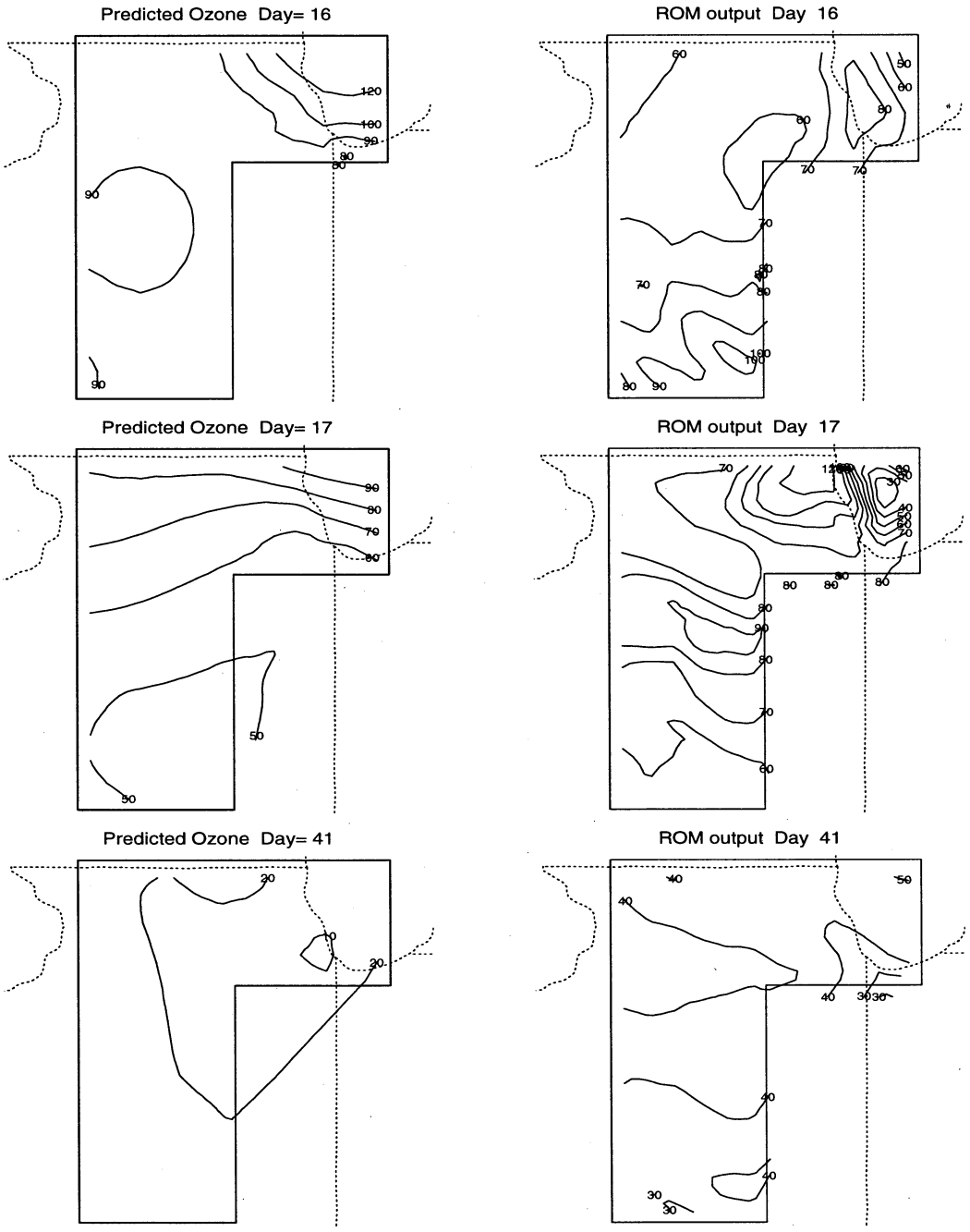

Figure 5: ROM and predicted ozone surfaces for days 16, 17 and 41.

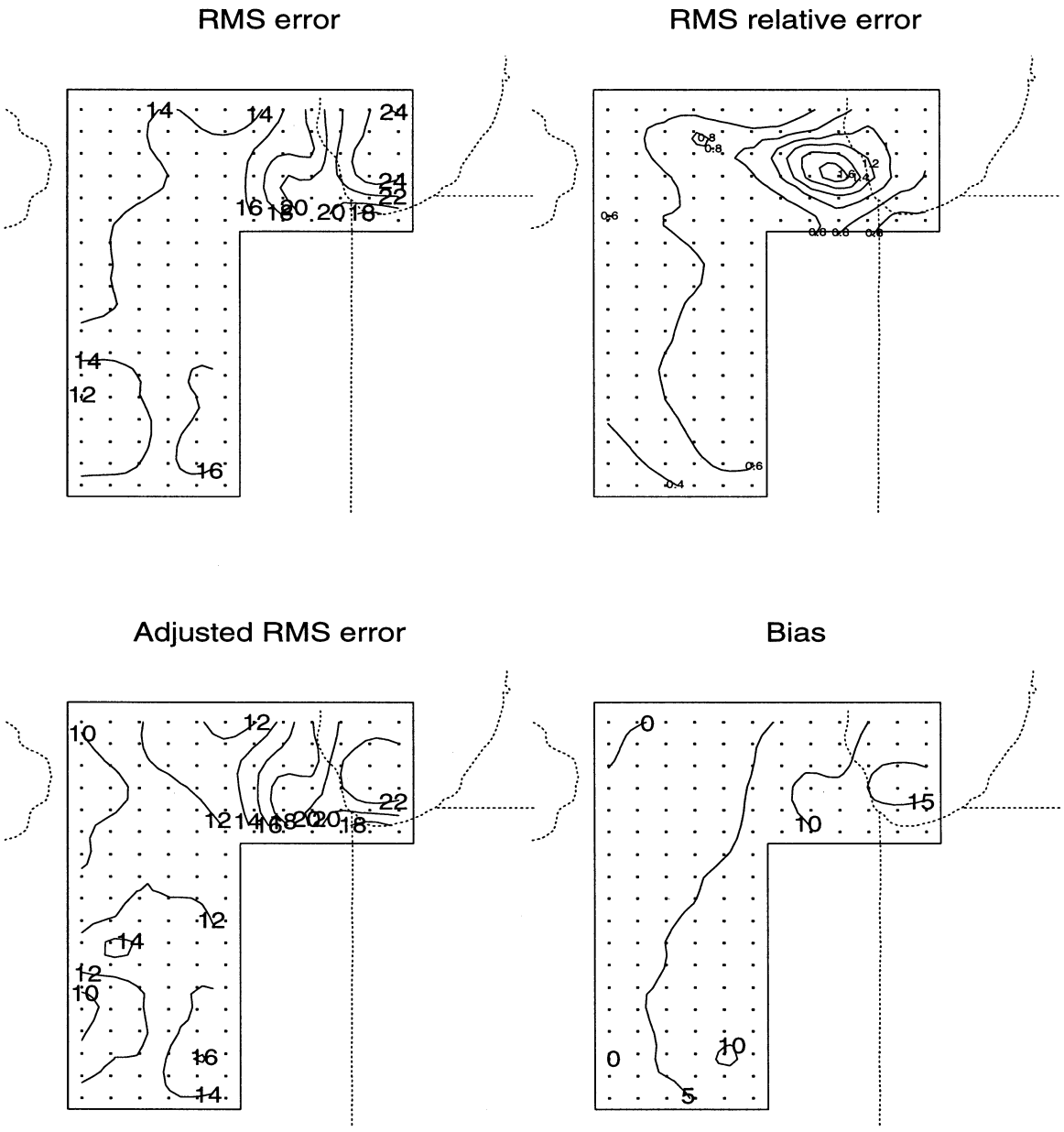

Figure 6: Root mean squared errors of the grid cells as a function of spatial location.

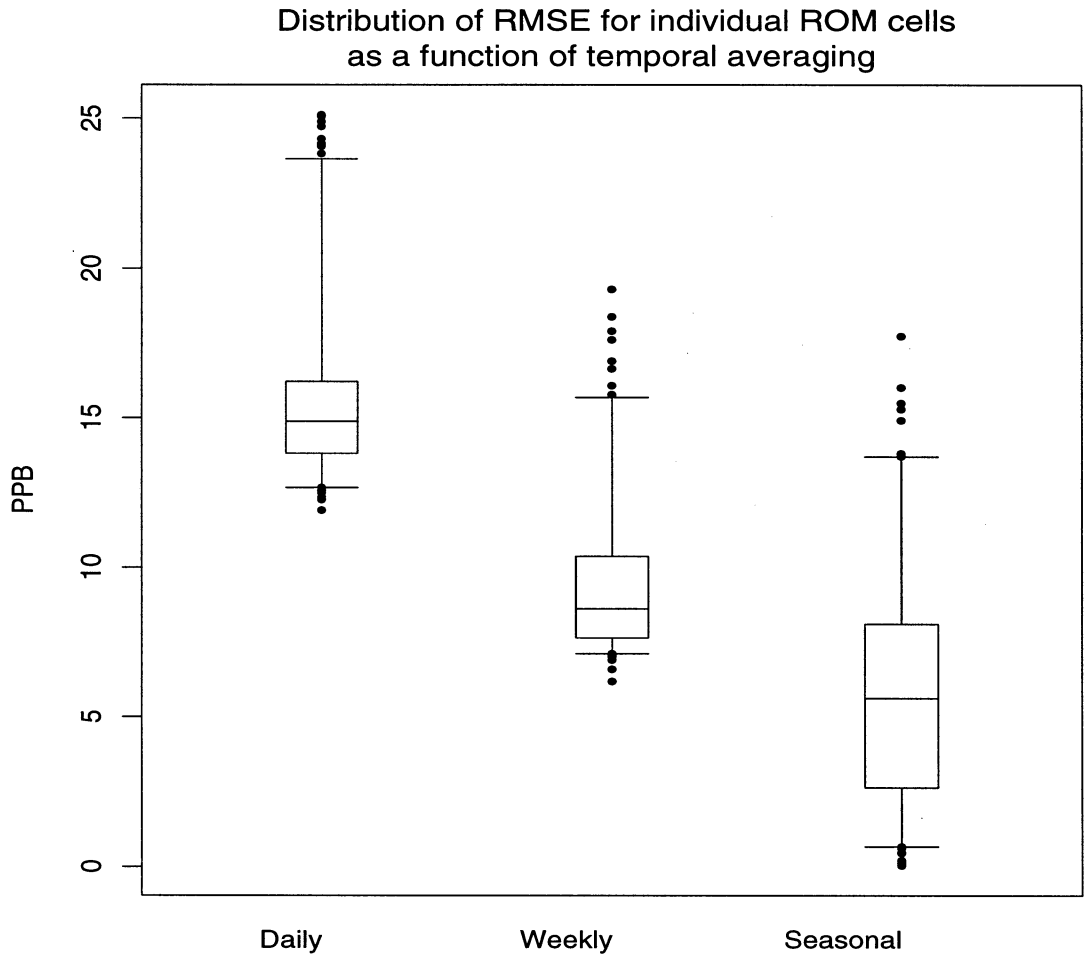

Figure 7: The distribution of root mean squared errors for the grid cells at three levels of temporal averaging.

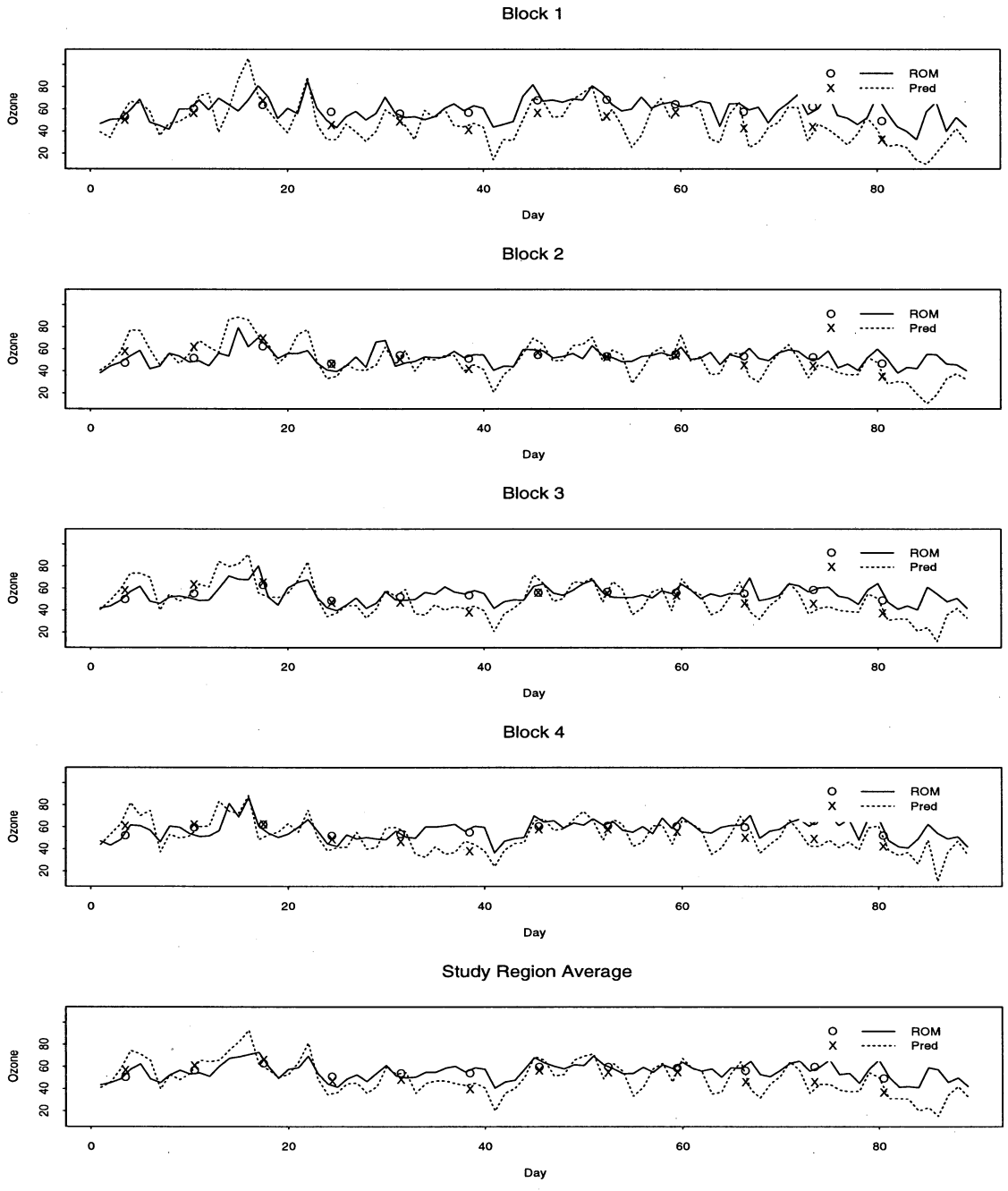

Figure 8: Time plots of block and study region averages.

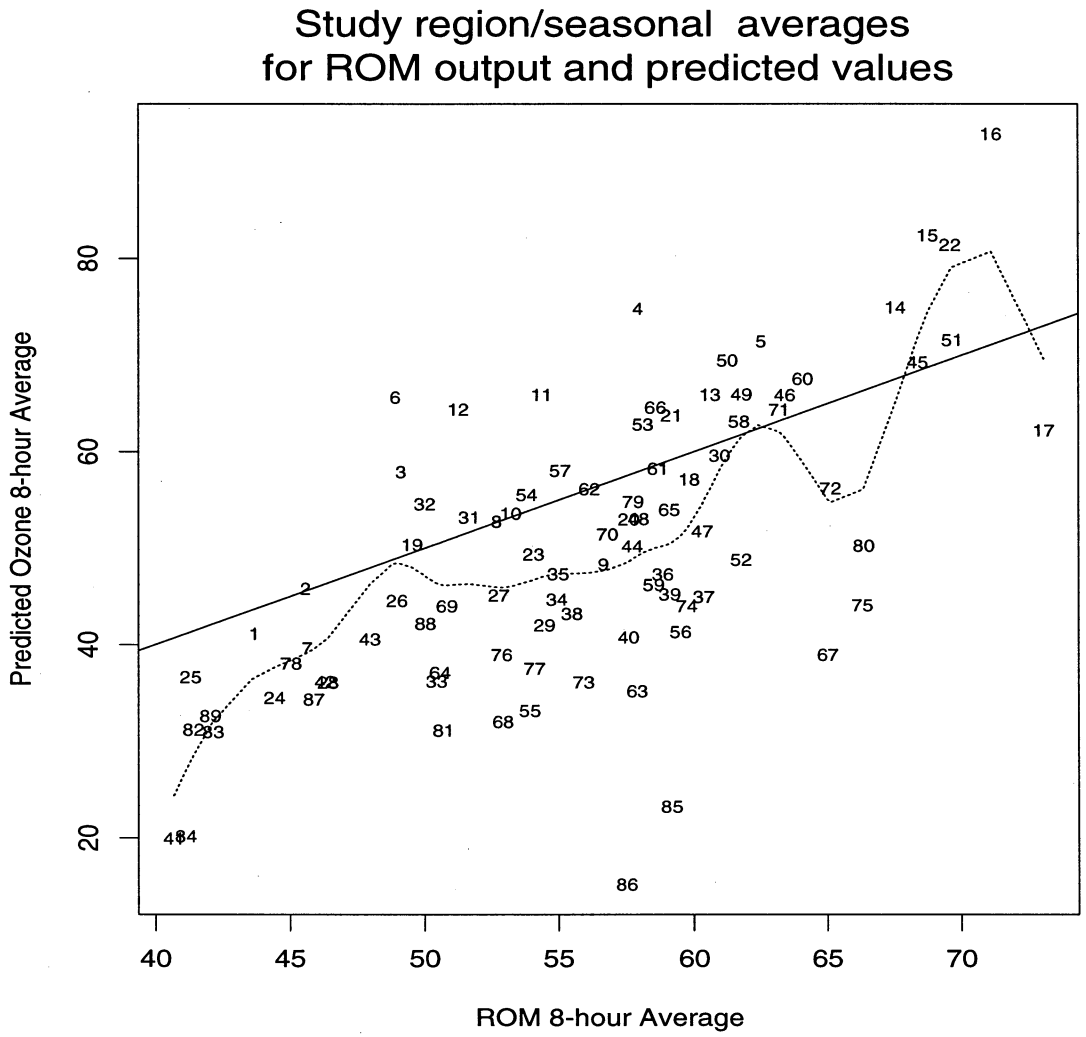

Figure 9: Scatterplot of ROM and predicted averages for the study region.

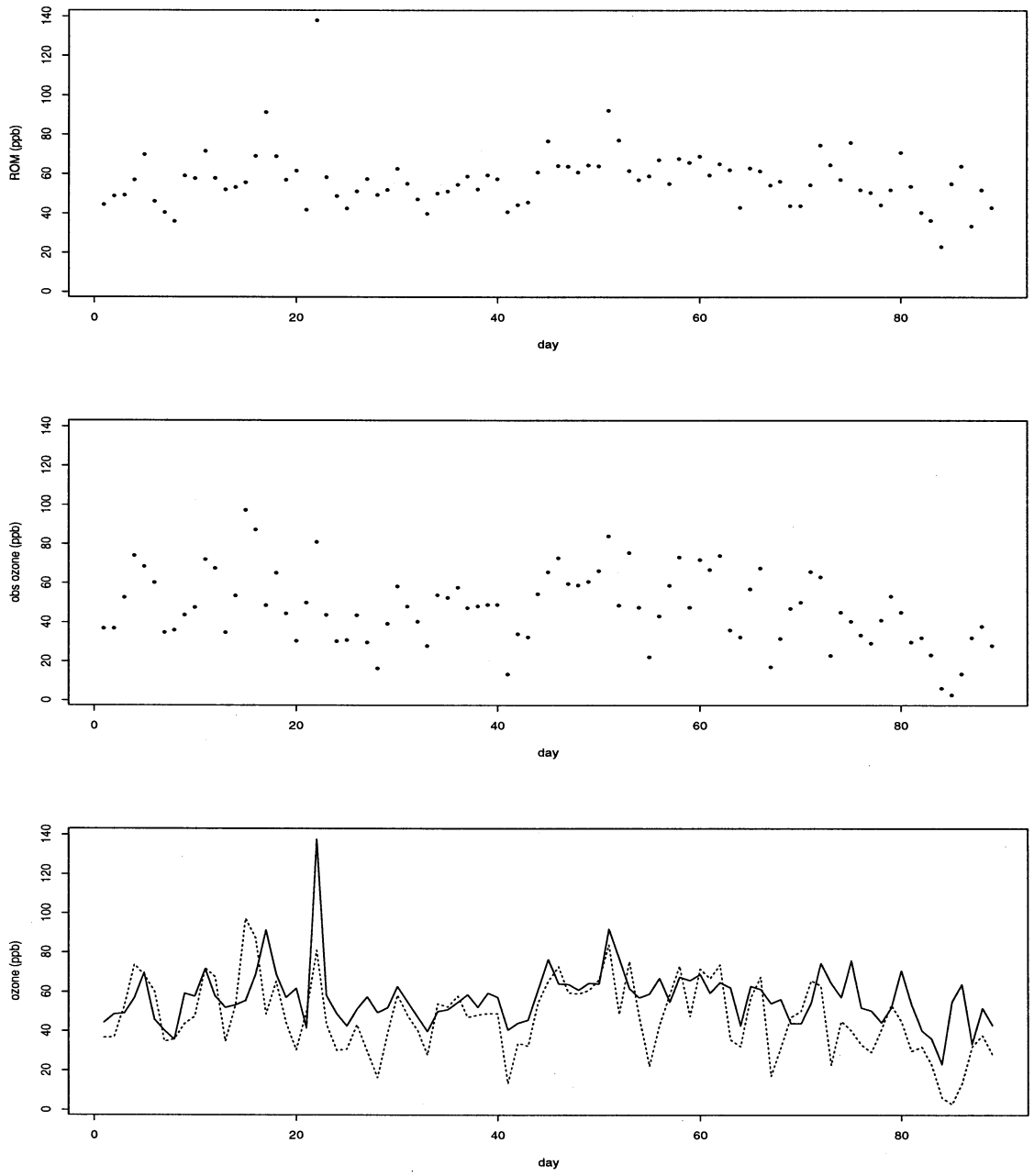

Figure 10: Top: daily (8-hr average) ROM predictions for the Chicago case. Middle: daily (8-hr average) observed ozone. Bottom: top two plots superimposed with lines connecting points. ROM predictions are indicated by the solid line.

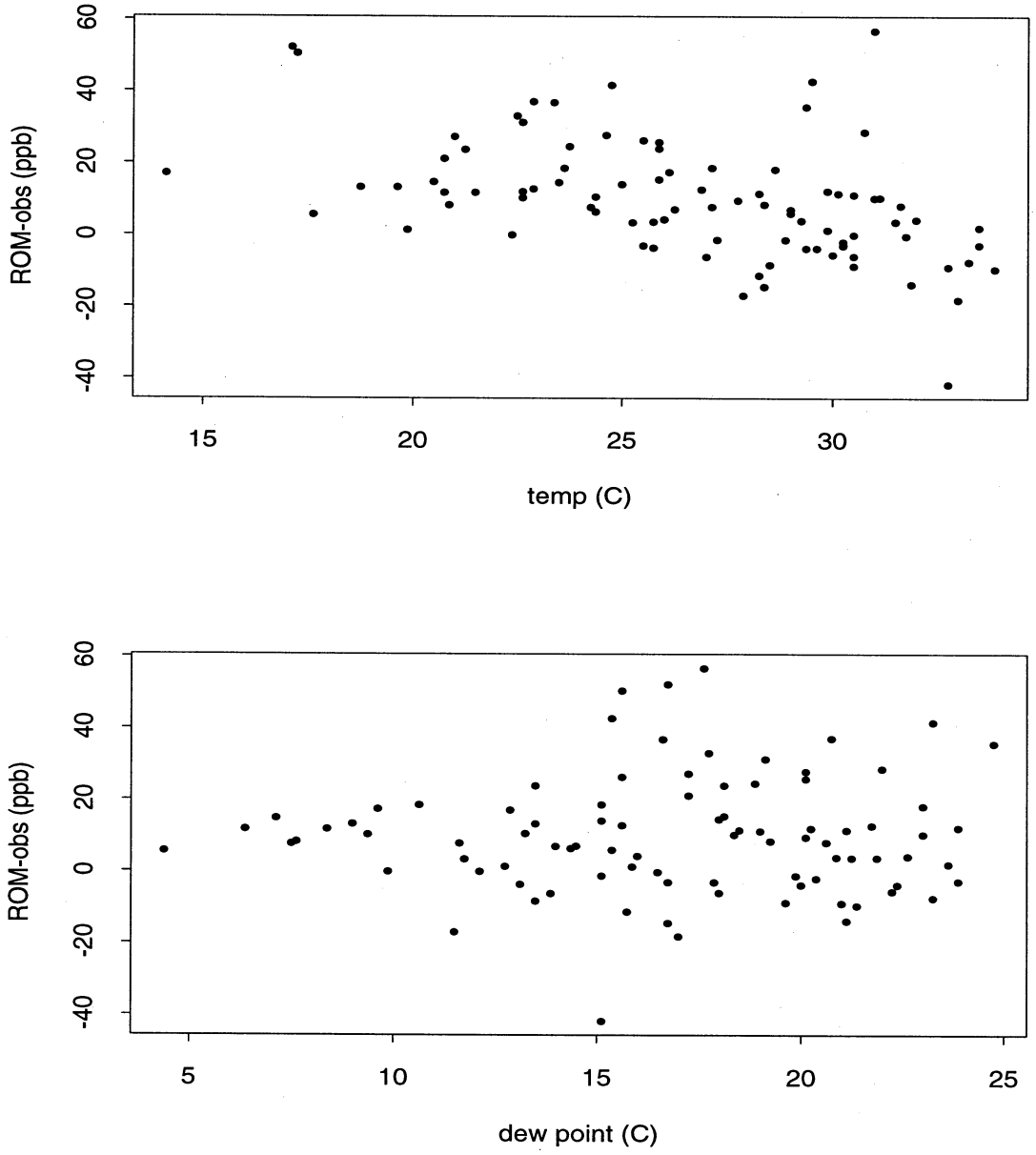

Figure 11: Daily ROM predictions minus daily observed ozone plotted against daily temperature and dew point temperature at Chicago.

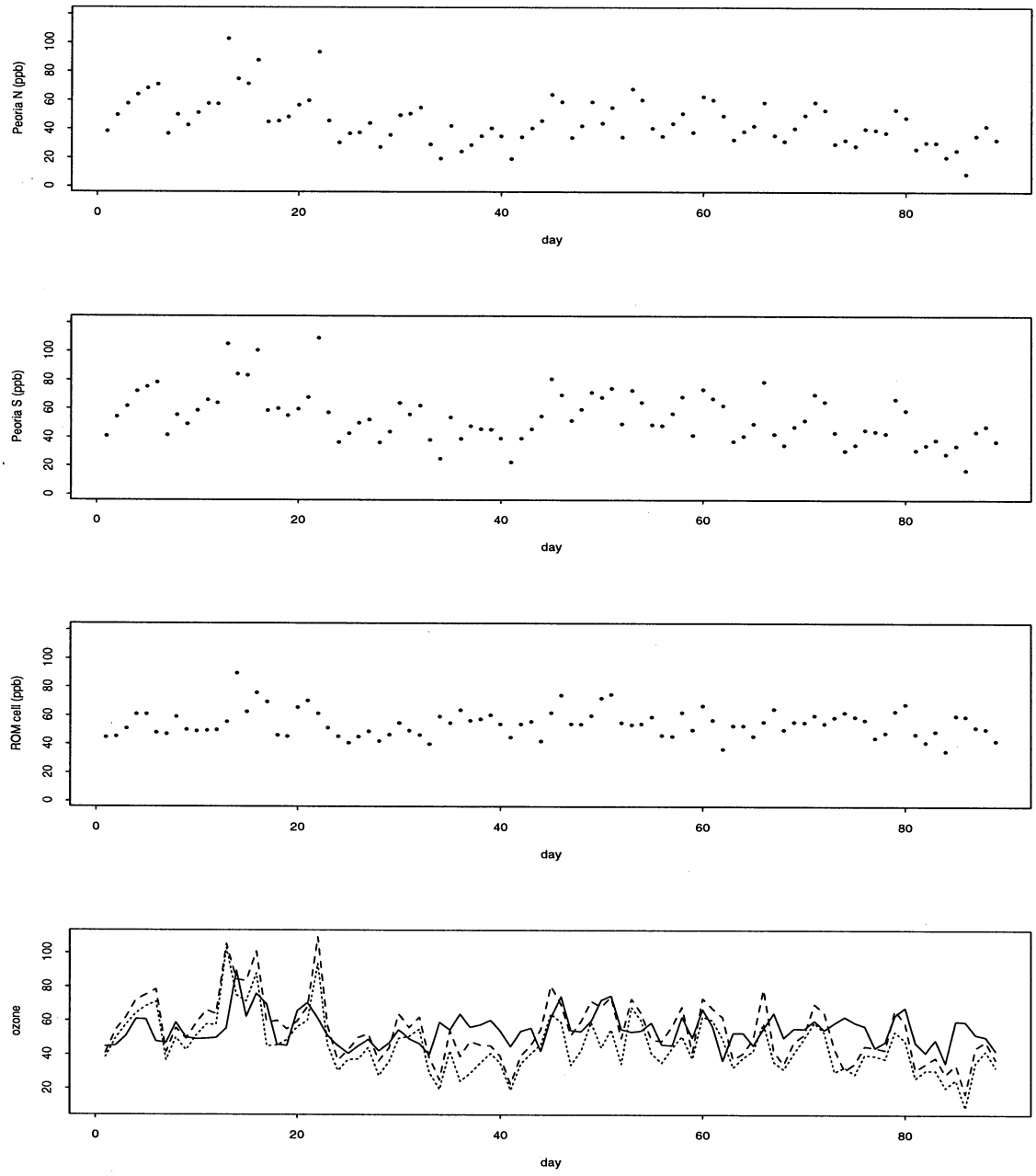

Figure 12: Time plots of observed ozone and ROM output for Peoria. First two plots are daily observed ozone for the north Peoria station and daily observed ozone for the south Peoria station, respectively. Third plot is daily ROM ozone predictions. The last plot is an overlay of all three time series. The ROM data are indicated by the solid line.

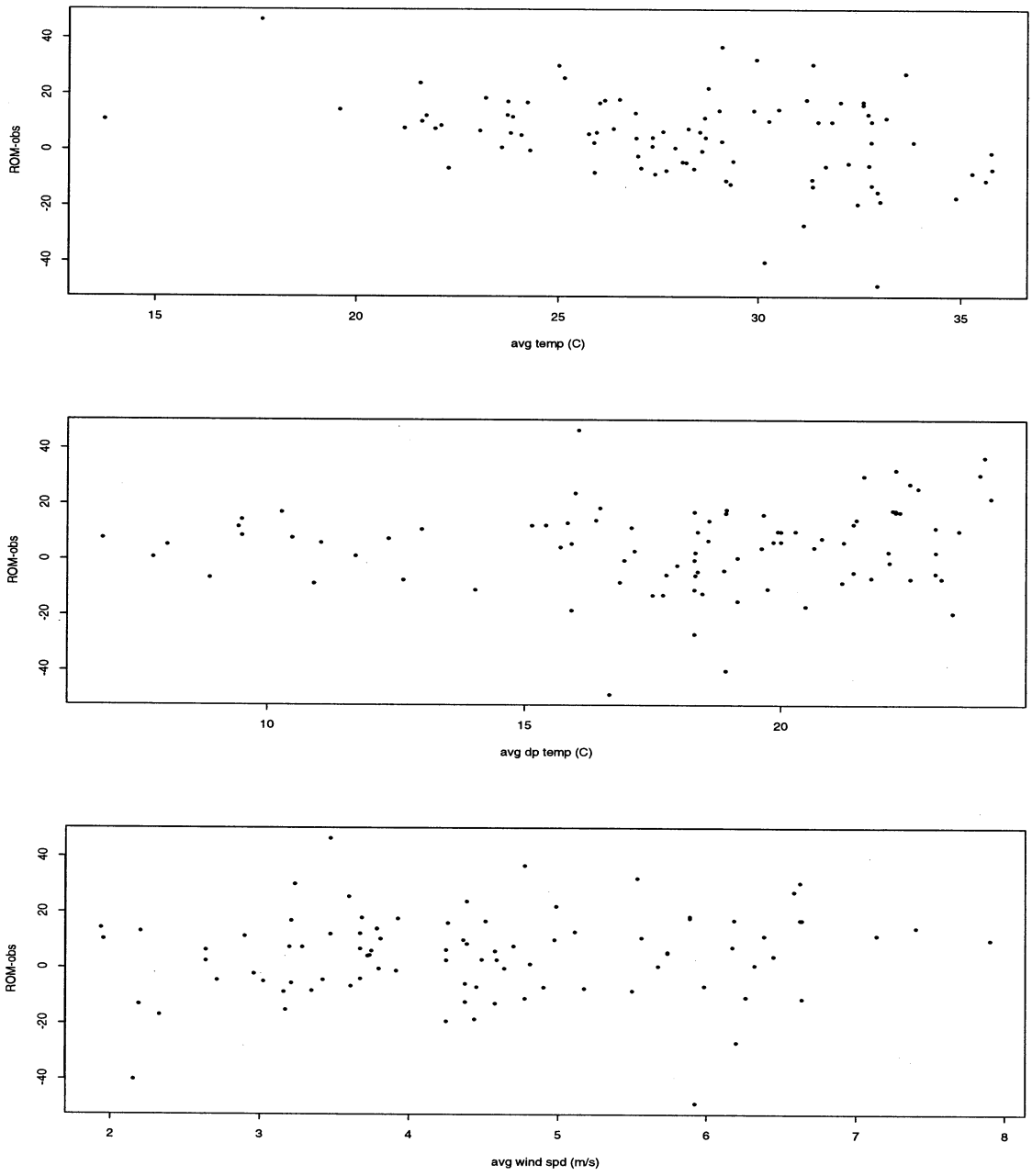

Figure 13: Top: Daily ROM predictions minus daily observed ozone (from combined north and south observed ozone) plotted against daily temperature for Peoria. Middle: Daily ROM predictions minus daily observed ozone (from combined north and south observed ozone) plotted against daily dew point temperature. Bottom: Daily ROM predictions minus daily observed ozone (from combined north and south observed ozone) plotted against daily wind speed.

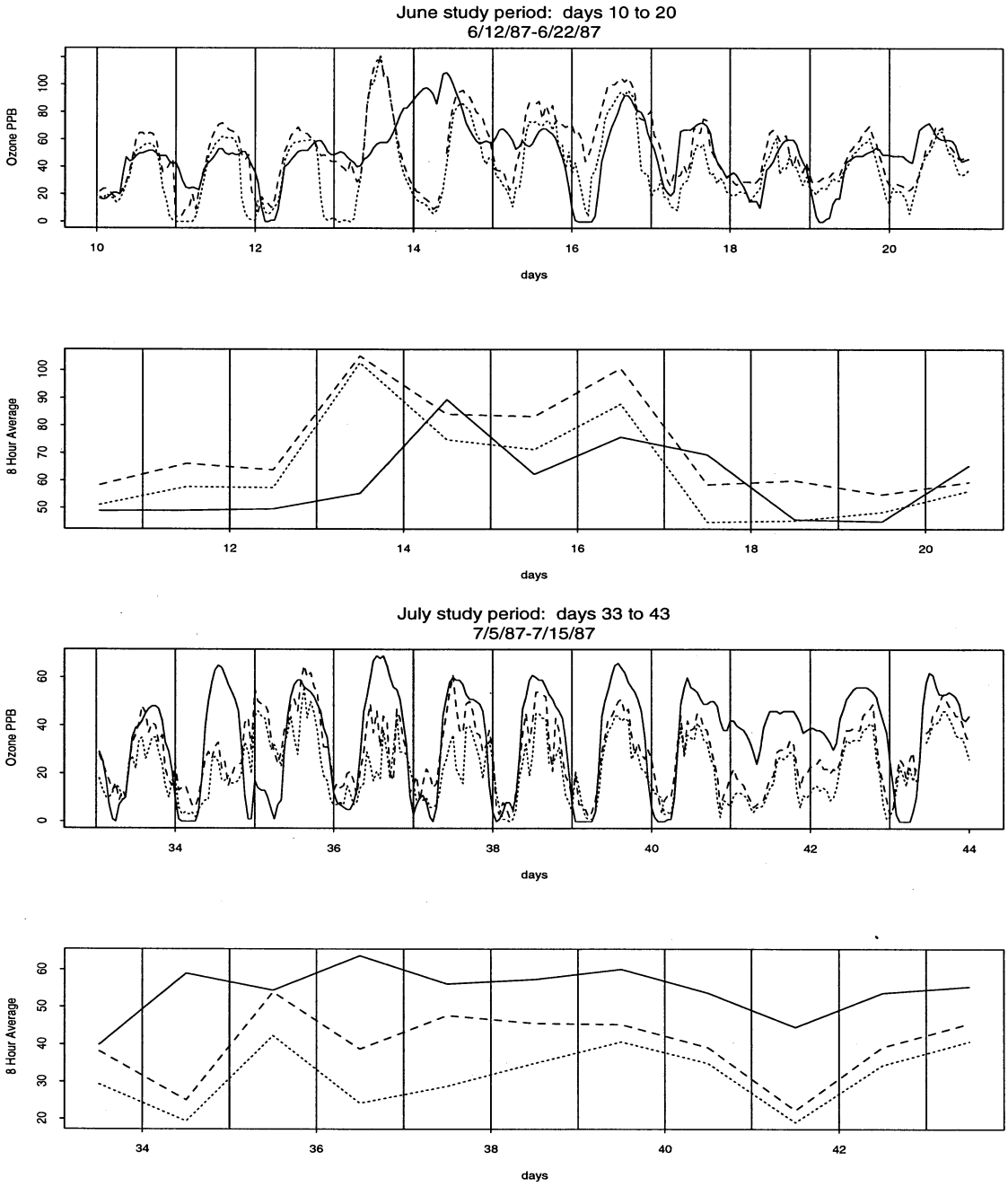

Figure 14: First Panel: Hourly observed ozone (dashed lines) for two stations (see Figure 1) and ROM data for days 10-20 (12-22 June) at Peoria. ROM is the solid line. Second Panel: The 8-hr averages for the first panel. Third Panel: Hourly observed ozone and ROM data for days 33-43 (5-15 July) at Peoria. Fourth Panel: The 8-hr averages for the third panel.

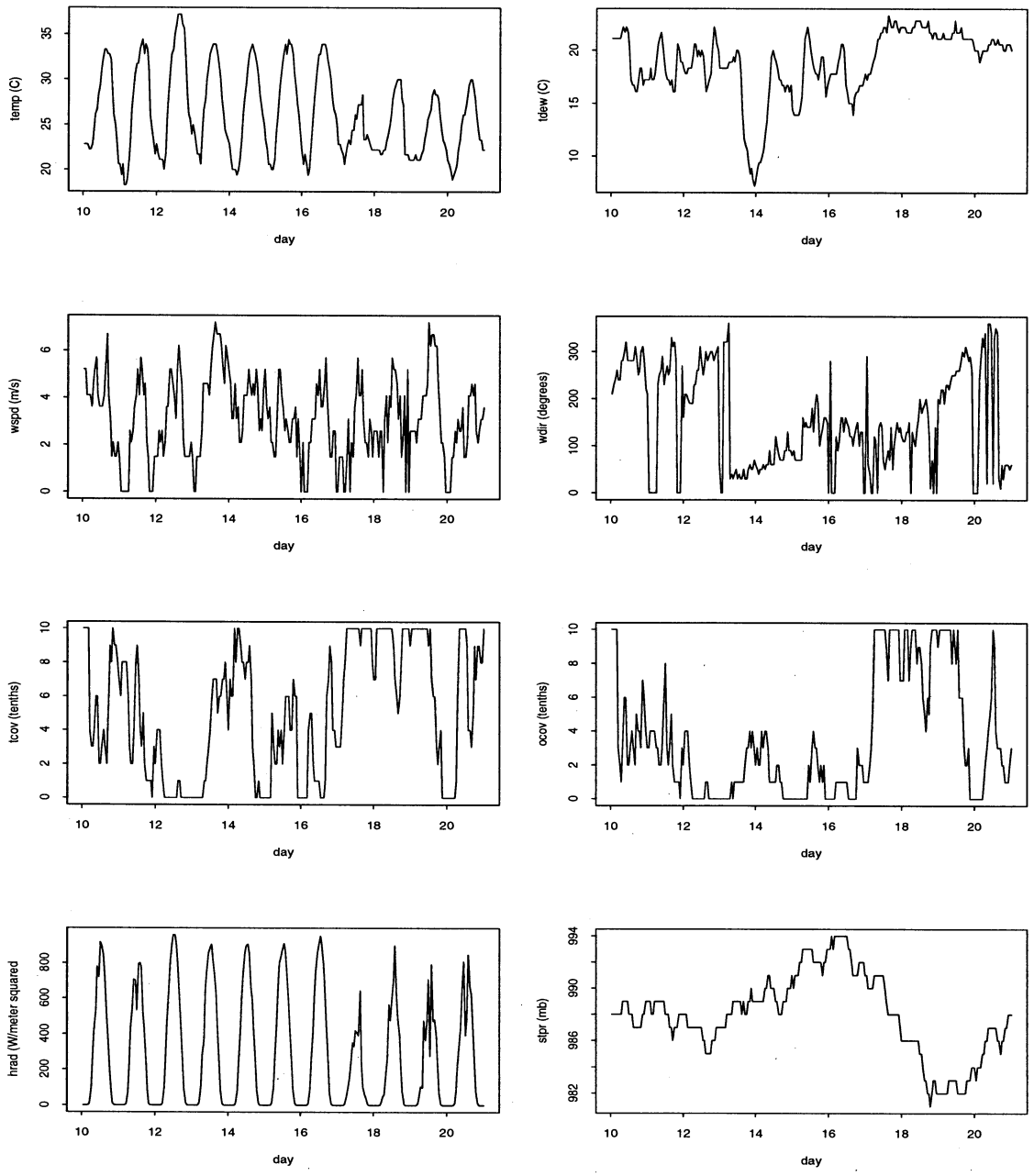

Figure 15: Hourly meteorological data for days 10-20 (12-22 June) at Peoria. Variables shown are temperature, dew point, wind speed, wind direction, total cloud cover, opaque cloud cover, total solar radiation and station pressure.

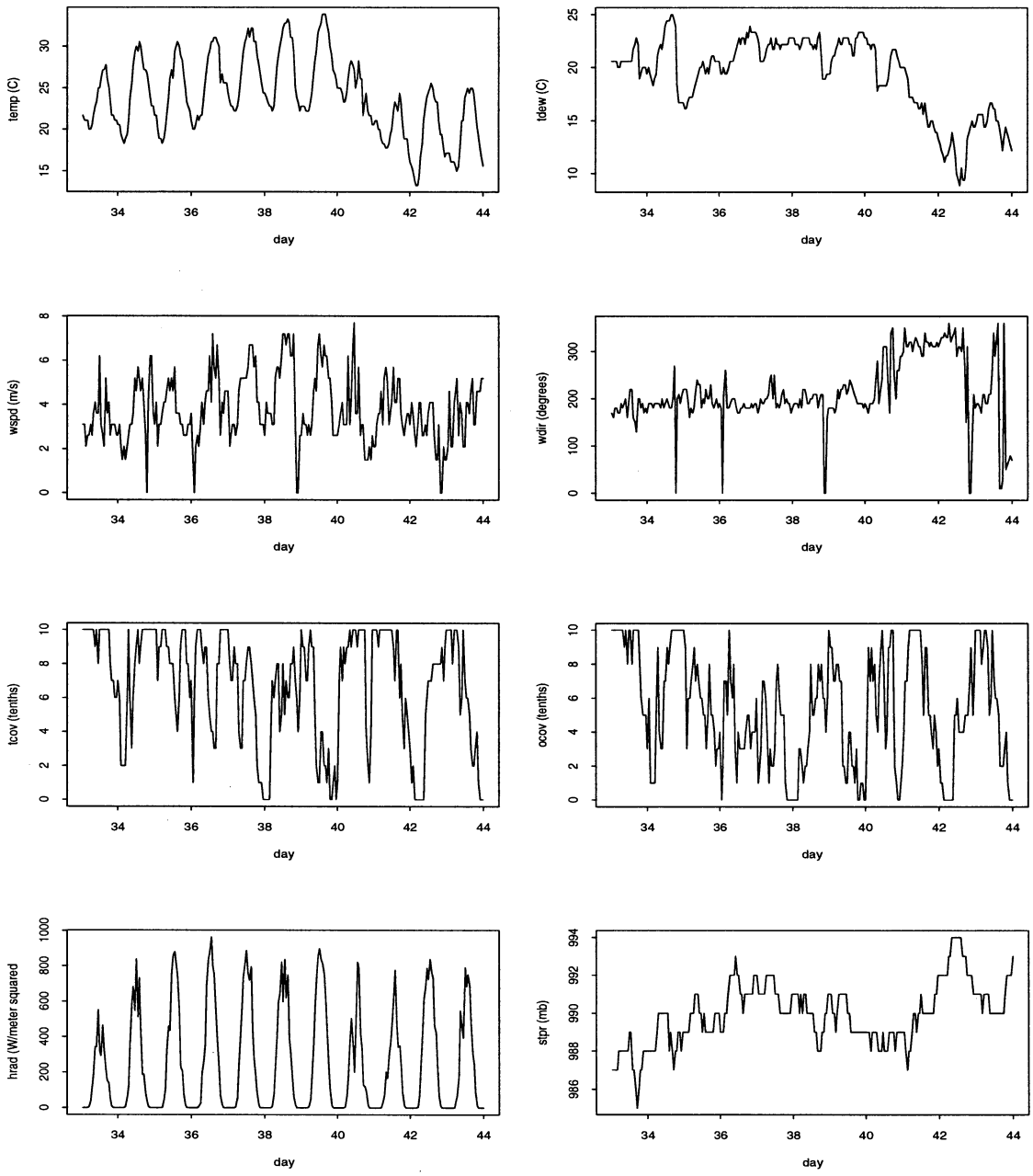

Figure 16: Hourly meteorological data for days 33-43 (5-15 July) at Peoria. Variables shown are temperature, dew point, wind speed, wind direction, total cloud cover, opaque cloud cover, total solar radiation and station pressure.